Journal of Applied Polymer Science

A comparison of partially acetylated nanocellulose, nanocrystalline cellulose, and nanoclay as fillers for high-performance polylactide nanocomposites

Jon Trifol,[1] David Plackett,[2] Cecile Sillard,[3] Ole Hassager,[1] Anders Egede Daugaard,[1] Julien Bras,[3] Peter Szabo[1]

[1]Department of Chemical and Biochemical Engineering, Danish Polymer Centre, Søltofts Plads, Building 229, DK - 2800 Kgs, Lyngby, Denmark

[2]Faculty of Pharmaceutical Sciences, University of British Columbia, 2405 Wesbrook Mall, Vancouver, BC, V6T 1Z3, Canada

[3]Université Grenoble Alpes, LGP2, F-38000 Grenoble, France CNRS, LGP2, F-38000 Grenoble, France

Correspondence to: P. Szabo (E-mail: ps@kt.dtu.dk)

ABSTRACT: Partially acetylated cellulose nanofibers (CNF) were chemically extracted from sisal fibers and the performance of those CNF as nanofillers for polylactide (PLA) for food packaging applications was evaluated. Three PLA nanocomposites; PLA/CNF (cellulose nanofibers), PLA/CNC (nanocrystalline cellulose), and PLA/C30B (Cloisite™ 30B, an organically modified montmorillonite clay) were prepared and their properties were evaluated. It was found that CNF reinforced composites showed a larger decrease on oxygen transmission rate (OTR) than the clay-based composites; (PLA/CNF 1% nanocomposite showed a 63% of reduction at 23°C and 50% RH while PLA/C30B 1% showed a 26% decrease) and similar behavior on terms of water vapor barrier properties with 46 and 43%, respectively of decrease on water vapor transmission rate at 23°C and 50% RH (relative humidity). In terms of mechanical and thermomechanical properties, CNF-based nanocomposites showed better performance than clay-based composites without affecting significantly the optical transparency. © 2015 Wiley Periodicals, Inc. J. Appl. Polym. Sci. **2016**, *133*, 43257.

KEYWORDS: barrier properties; cellulose nanofibers (CNF); microfibrillated cellulose; nanoclays; polylactic acid

Received 26 August 2015; accepted 19 November 2015

DOI: 10.1002/app.43257

INTRODUCTION

The use of petrochemical products for packaging applications represents a serious global environmental challenge, not only from the point of view of the availability of the raw material but also due to disposal of the products. For that reason in recent years, especially in the packaging industry, a considerate effort has been made in order to develop both biobased and biodegradable materials to substitute the materials that are being used currently (e.g., PE and PET). The use of biobased and biodegradable polymers such as polylactide (PLA) is finding an increasing number of applications which has led to perspectives of high growing in production and market.[1,2] Traditionally, PLA has been deemed to have inferior material performance compared to the most widely used synthetic polymers for which it might substitute. In particular, poor thermomechanical properties, brittleness, slow crystallization, medium oxygen, and water vapor barrier properties have been some of the major technical obstacles in expanding applications for PLA.[3]

To improve the properties of PLA, several different strategies have been adopted. These strategies include modifying PLA (e.g., block copolymers),[4] blending with other polymers such as PEG, use of reinforcing agents such as natural fibers,[5] nanoclays,[6] nanocellulose,[7] chitosan,[8] xylans,[9] and calcium carbonate[10] among others. Cellulose nanofibers (CNF) or cellulose nanocrystals (CNC), which can be obtained from lignocellulosic materials or from bacteria or algae,[11,12] have received the attention of numerous researchers not only for their biodegradability, bio-based origin, and availability but also due to their good reinforcing properties[13] which makes it a promising nanofiller for PLA. There are already several reports on PLA/CNF nanocomposites,[14–16] with various results reported. The reason for such variations might be the large number of parameters involved in the reinforcing effect, such as the quality of the

Additional Supporting Information may be found in the online version of this article.

reinforcing agent (aspect ratio/yield), the dispersion of the filler in the matrix, and the presence of aggregates amongst others.

The mechanical properties of PLA/nanocellulose composites have been widely studied, and while in one hand there are reports claiming a great reduction in the tensile strength and Young modulus 47%,[17] in the other hand there are other works reporting a slight improvement of the mechanical properties,[18] but, generally, the reinforcing of CNF is more pronounced at temperatures above the T_g, when the mechanical resistance of the polymer dramatically decreases. In food packaging applications, good thermomechanical stability is required not only for special applications such as microwave heated food, but also for processes such as thermoforming.

Apart from the thermomechanical properties, the barrier properties are critical for some food packaging applications. For example, oxygen can enhance microbiological activity and oxidize the food; water vapor ingress can lead to deterioration of dry products and aroma barrier properties may also be required. Although a frequent reference material for barrier properties is PET, implying that the OTR of PLA should be decreased by 90%, there is a huge range of food packaging applications (i.e., MAP (modified atmosphere packaging), poultry product packaging, vegetable packaging, and so on), where any kind of improvement in barrier properties of PLA could make this material useful, even if the improvement in barrier properties does not reach the same level as PET.

In theory, nanofillers such as C30B increase the so-called tortuous path through a polymer film, meaning that gas or water molecules passing through the films have to follow a longer path, so, diffusivity and hence permeability are thereby reduced. The studies on the effect of CNF on the barrier properties of PLA show also a large variation. From a decrease of 90% in the oxygen permeability at 75% RH on PLA/CNC 2% films[17] to moderate improvements (9–43%)[16] and finally there are reports of a reduction on both oxygen and water barrier properties.[19] Finally, nanocellulose has been reported to have a nucleating agent behavior[18,20] of PLA.

A key point to obtain enhanced properties of PLA/CNF nanocomposites is to achieve a very good dispersion of nanofillers in the polymer matrix. The dispersion of hydrophilic nanocellulose within a hydrophobic still remains a challenge, and some strategies such as the use of surfactants[21] or grafting hydrophobic chains onto nanocellulose surface[22] are usually required in order to achieve good dispersion. In previous publications a method to produce high yield partially acetylated-CNF by means of chemical methods was developed.[23] Because of the high yield and the partially grafted nature of those nanofillers they may be promising additives to enhance the performance of PLA for food packaging applications.

The aim of this work is to compare the performance of those CNF not only with the neat PLA, but also with CNC and clay. From the diverse amount of clay, such as montmorillonite,[24] kaolin,[25] the C30B, a commercially available organically modified clay, was selected, since it has been widely used to reinforce PLA, increasing the tensile modulus by 13% and impact strength by 27% at 3% load,[26] 63% the tensile modulus at 5% load,[27] and by decreasing the water vapor permeability by 40% at 5% load.[28]

EXPERIMENTAL

Materials and Methods

L-polylactide (Ingeo 2003D) was kindly supplied by Natureworks (Minnesota, MN). Nanocellulose was extracted from sisal which was kindly supplied by Expor Sisal S.L. The chosen nanoclay was the commercially available Cloisite 30B which is reported to have a cationic exchange capacity (CEC) of 90[29] and a tetraalkyl ammonium salt as a surfactant modifier. NaOH, sulfuric acid (95–97%), nitric acid (ACS reagent, 70%), acetic acid (99–100%), *N*,*N*-dimethyl formamide (98%, ACS reagent) and dichloromethane (99, 8% chromasolv) were purchased from Sigma–Aldrich and sodium chlorite (25% w/w aqueous solution) from Merck. All of the reagents were used as received.

The thickness of cast PLA films (12 × 12 cm^2) was determined using a digital micrometer with a tolerance of ±1% at nine points (eight points on the edges and one in the middle). Films were examined microscopically to check for bubbles or other contamination and discarded if not deemed suitable for use.

The dispersion of the nanofiller in the matrix was studied by X-ray diffraction (XRD) using a Philips X'Pert Pro diffraction system containing a Cu tube ($\lambda = 1.542$ Å) operating at 40 kV and 40 mA. TEM (FEI Tecnai T20 G2) and SEM (FEI Helios EBS3, FEI Inspect) operating at 200 and 5 kV, respectively were also employed.

Thermal properties such as glass transition (T_g), melting temperature (T_m), and degree of crystallinity (X_c) of PLA and the nanocomposites were determined by DSC (TA DSC Q1000) with heating and cooling rates of 10°C min^{-1} in a range of 0–200°C in a heat/cool/heat cycle. A melting enthalpy (ΔH_0) of 93 J g^{-1} for 100% crystalline L-polylactide) was used as reported by Ref. 30. To determine X_c for the first and second heating cycles eq. (1) was used.

$$Xc = \frac{1}{1 - M_{NF}} \frac{\Delta H_m - \Delta H_C}{\Delta H_0} \quad (1)$$

Where X_c is the degree of crystallinity of the composite, M_{NF} the content of nanofiller, ΔH_m is the melting enthalpy (the area of the peak which minimum is at T_m) and ΔH_C is the crystallization enthalpy.

The isothermal crystallization studies were conducted using the following cycle: heating at 10°C min^{-1} to 200°C, hold at 200°C for 2 min and cooled down to 0°C at 20°C min^{-1}. Subsequently, each sample was heated at 20°C until 120°C and then held at that temperature for 2 h. Finally, the samples were cooled to 0°C at 10°C min^{-1} and heated until 200°C at 10°C min^{-1}.

The spherulite size and shape of the nanocomposites due to the solvent casting approach was compared with the crystallinity induced by isothermal crystallization. The neat PLA and the nanocomposites were placed between two microscope crystal slides and introduced in a heating device connected to an

optical microscope with polarized light. The samples were heated until 200°C for 2 min and thereafter were cooled to room temperature using a tissue impregnated with ethanol. Finally the samples were introduced in the heating chamber at 100°C and the crystallization process was recorded by a camera.

The optical properties were measured at least at three different points on each cast film using a UV–vis spectrometer (Polar Star Omega) in the range of 200–1000 nm.

The oxygen transmission rate (OTR) was measured in triplicate sample sets using a Lyssy OPT-5000 Oxygen permeability tester. Experiments were performed at 23°C at 0% or 50% RH. Results were expressed in units of mL μm m^{-2} day^{-1}.

The water vapor transmission rate (WVTR) of the films was measured in triplicate sample sets according to the norm NF H 00-030[22] at 23°C and 50% RH using silica gel as desiccating agent with a specific exchange surface (S) 28.27 cm^2. The mass increase of the cups, due to the water absorption of silica gel was plotted against time having slope n. The WVTR was calculated with eq. (2) in which l is the thickness of the film.

$$\mathrm{WVTR} = \frac{n * l}{S} \tag{2}$$

The mechanical properties of sample films were measured in an Instron Universal Testing Machine Model 4507 (Instron Engineering Corporation, Canton, MA) equipped with pneumatic jaws of type I BA using dumbbell-shaped samples. The properties were measured at a strain rate of 2.5 mm min^{-1}. This testing was carried out using five 5 × 1 cm^2 samples from each film type after thickness measurement at four locations. The samples were preconditioned at 23°C and 50% RH.

The thermomechanical properties of test films were measured in duplicate samples using a DMA RSA3 (TA Instruments, USA) equipment working in tensile mode. The measurements were performed at a constant frequency of 1 Hz and strain amplitude of 0.05% with a distance between jaws of 10 mm. The samples were heated at 10°C min^{-1} from room temperature to 110°C, were held at this temperature for 20 min and then cooled to 25°C at 10°C min^{-1}. In a final step, the samples were heated to 180°C at 10°C min^{-1}. The analysis of each sample was carried twice to check the reproducibility of the measurements.

Preparation of CNF and CNC

CNF Preparation. Our method for isolation of the cellulose nanofibers (CNF) has been already discussed.[23] The method consists of a sequence of chemical treatments to sisal fibers:

A. *Washing*: 50 g of sisal fibers (S) of around 200 μm of diameter, were cut to ~2 cm of length, and washed with 1.5 L of a solution of 2% NaOH at room temperature overnight in a 2-L round bottom flask. After that the fibers were filtered and washed, adding distilled water until no further change was observed in the pH of the aqueous suspension
B. *Mercerization (SM)*: After that the washed fibers were collected and treated with 1.5 L of a solution of NaOH at 10% in a 2-L round bottom flask and were held for 1.5 h at boiling temperature. This procedure was repeated two more times and the fibers were washed.
C. *Bleaching (SMB)*: The mercerized pulp (SM) collected in 1.25 L of distilled water in a 2-L round bottom flask and the temperature was raised to 70°C. Once this temperature was achieved, 10 mL of acetic acid and 50 mL of $NaClO_2$ were added once per hour for the next 7 h. Finally, the bleached pulp was filtered and cleaned until no change in the pH was observed.
D. *Acetylation (SMBA)*: The bleached pulp (SMB) was collected in a 2-L round bottom flask with 150 mL of nitric acid and 900 mL of acetic acid. This solution was kept at boiling temperature and magnetic stirring for 90 min and after that, the reaction medium was cooled by diluting with cold water (ratio 1:5).

This pulp was submitted either for a dispersion-centrifugation procedure to achieve CNF or to acid hydrolysis to achieve CNW.

1. *CNF isolation*: To extract and individualize CNF, the SMBA was washed with DMF and solvent exchanged into DMF three times with no intermediate redispersion to be finally diluted with DMF until achieve a solution of 1% of CNF on DMF. This mixture was kept under vigorous magnetic stirring for 3 days and then was centrifuged (~2500 rpm for 10 min) to separate the individualized nanofibers from the remaining aggregates. The supernatant was collected and the precipitate—remaining aggregates—was discarded.
2. *CNC isolation*: CNC were obtained by acid hydrolysis of SMBA. Nearly 20 g SMBA pulp was treated with 400 mL of 32% sulfuric acid at 45 °C for 2 h under magnetic stirring. The suspension was then diluted five-fold with water and dialyzed until no change in pH was observed. Finally, the product was solvent exchanged into DCM and thereafter to DMF. The CNC in DMF was held for 24 h under strong magnetic stirring and was then centrifuged to separate the aggregates (~1500 rpm for 10 min). The supernatant containing CNC was used to make the nanocomposites.

Preparation of Nanocomposites

Neat PLA film and three types of nanocomposites: (a) PLA/C30B; (b) PLA/CNF, and (c) PLA/CNC were prepared by solvent casting. Briefly, separately, PLA and nanofillers were dissolved/predispersed in a solvent, and thereafter the two solutions were mixed, casted in a Teflon mold and dried.

Neat PLA Film. For the neat PLA, 10 g of PLA were dissolved in 200 mL of DCM (dichloromethane) using magnetic stirring, overnight. After that, 100 mL of the DCM solution were poured in a 250 mL Erlenmeyer and the solution was raised until 250 mL by adding extra DCM. Thereafter, the suspension was degassed by ultrasonication for 5 min and 240 mL of that solution was poured slowly into three Teflon molds (80 mL/each mold). The three molds were covered by a 5- to 13-μm filter paper and they were kept in a Climacell climatic chamber (MMM Group) at 23°C for 16 h. Subsequently, the resulting PLA/C30B films were dried at 50°C under vacuum for a minimum of 24 h.

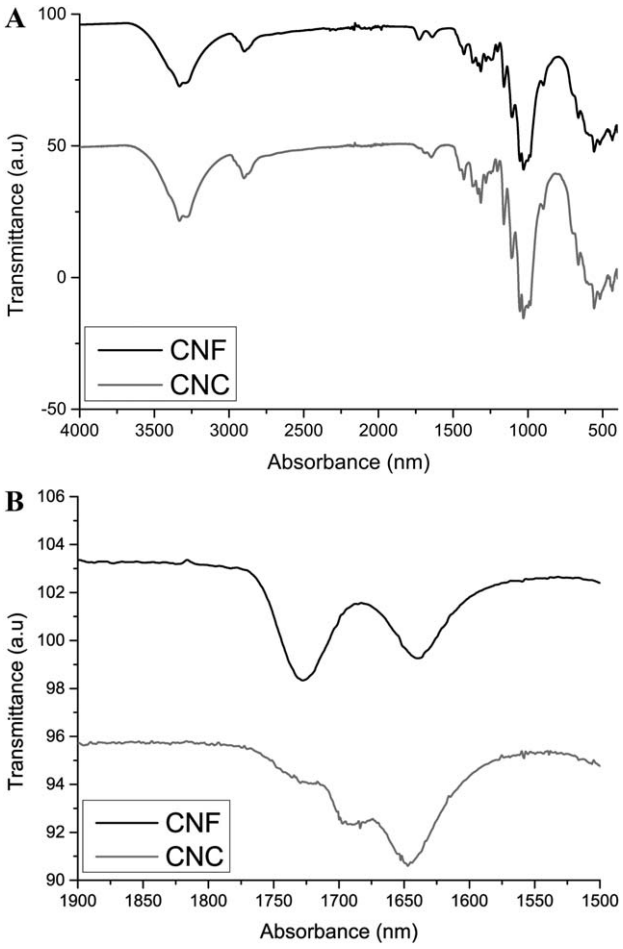

Figure 1. FT-IR of the CNC and CNF. Left: 4000–400 cm^{-1}; Right: Zoom 1900–1500 cm^{-1}.

PLA/C30B Nanocomposites. To prepare the C30B nanocomposites, first, the C30B was predispersed on DCM in the following way: 3.0 g of C30B were mixed with 300 mL of DCM and this mixture was magnetically stirred for 24 h. Thereafter, nanoclay suspension in a DCM solution was ultrasonicated for 3 h at 200W and homogenized for 90 min, which was found to be the optimal procedure for the clay dispersion, with an Ultraturrax homogenizer (Jonke & Kunnel IKA Ultraturrax T25) at 20,500 rpm.

Thereafter, the previously prepared PLA solution and the predispersed nanoclay suspension were mixed to obtain the desired concentration of C30B in PLA. After that, they were kept for 10 min under strong magnetic stirring, and finally, the volume was then increased to 250 mL with DCM. This solution was thereafter ultrasonicated for 90 min, homogenized for 30 min and the necessary DCM was added to increase the volume again to 250 mL. Finally, the suspension was degassed by ultrasonication for 5 min and 240 mL of the solution was poured slowly into three Teflon molds (80 mL/each mold). The three molds were covered by a 5–13 μm filter paper and they were kept in a Climacell climatic chamber (MMM Group) at 23°C for 16 h. Subsequently, the resulting PLA/C30B films were dried at 50°C under vacuum for a minimum of 24 h.

PLA/CNF and PLA/CNC Nanocomposites. To elaborate nanocellulose-based composites, several solvents (water, acetone, dichloromethane (DCM), tetrahydrofuran (THF), dimethylformamide (DMF), dimethylacetamide (DMAc), and *N*-methyl-2-pyrrolidone (NMP)) were evaluated for PLA/nanocellulose film preparation, and after evaluating different aspects, it was found that DMF was the most suitable solvent for nanocellulose-based composites.

Nearly 3.3 g of PLA were dissolved in 66 mL of DMF by mixing and keeping them for 2 h at 70°C under vigorous stirring. After 2 h, the nanocellulose suspension on DMF, obtained in CNF/CNC isolation procedure, was added and the solution was increased to 100 mL with additional DMF. The PLA/nanocellulose mixtures were thereafter kept under vigorous stirring and ultrasonicated at 200 W for 10 min. Finally the solution was casted into two Teflon molds covered by a 5- to 13-μm filter paper (50 mL/each mold). In each case, remaining solvent was removed from cast films by drying at 80°C for 15 h followed by drying under vacuum at 50°C for 24 h.

Thermal Treatments. To achieve quenched nanocomposites, the films were hot pressed for 5 min at 170°C followed by a fast cooling in order to achieve essentially amorphous nanocomposites (AM). After that, to achieve fully crystallized nanocomposites, the quenched nanocomposites were placed into an oven at 120°C for 2 h in order to obtain fully crystallized nanocomposites (FC).

RESULTS AND DISCUSSION

The nanofillers were characterized by FT-IR and XRD as can be seen in Figures 1 and 2.

As can be clearly seen in Figure 1, there is a difference between the CNC and CNF FT-IR spectra at 1740 cm^{-1}. The CNF shows absorbance on the peak at 1740 cm^{-1}, corresponding to the carbonyl groups grafted onto the nanocellulose during the acetylation procedure that have been removed during the acid hydrolysis.

As can be seen in Figure 2, the crystallinity of the CNC and CNF are very similar, this is due to the fact that the acetylation

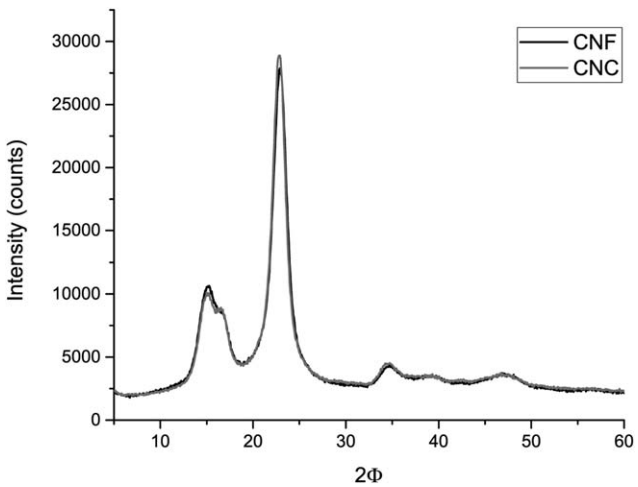

Figure 2. XRD patterns of CNF and CNC.

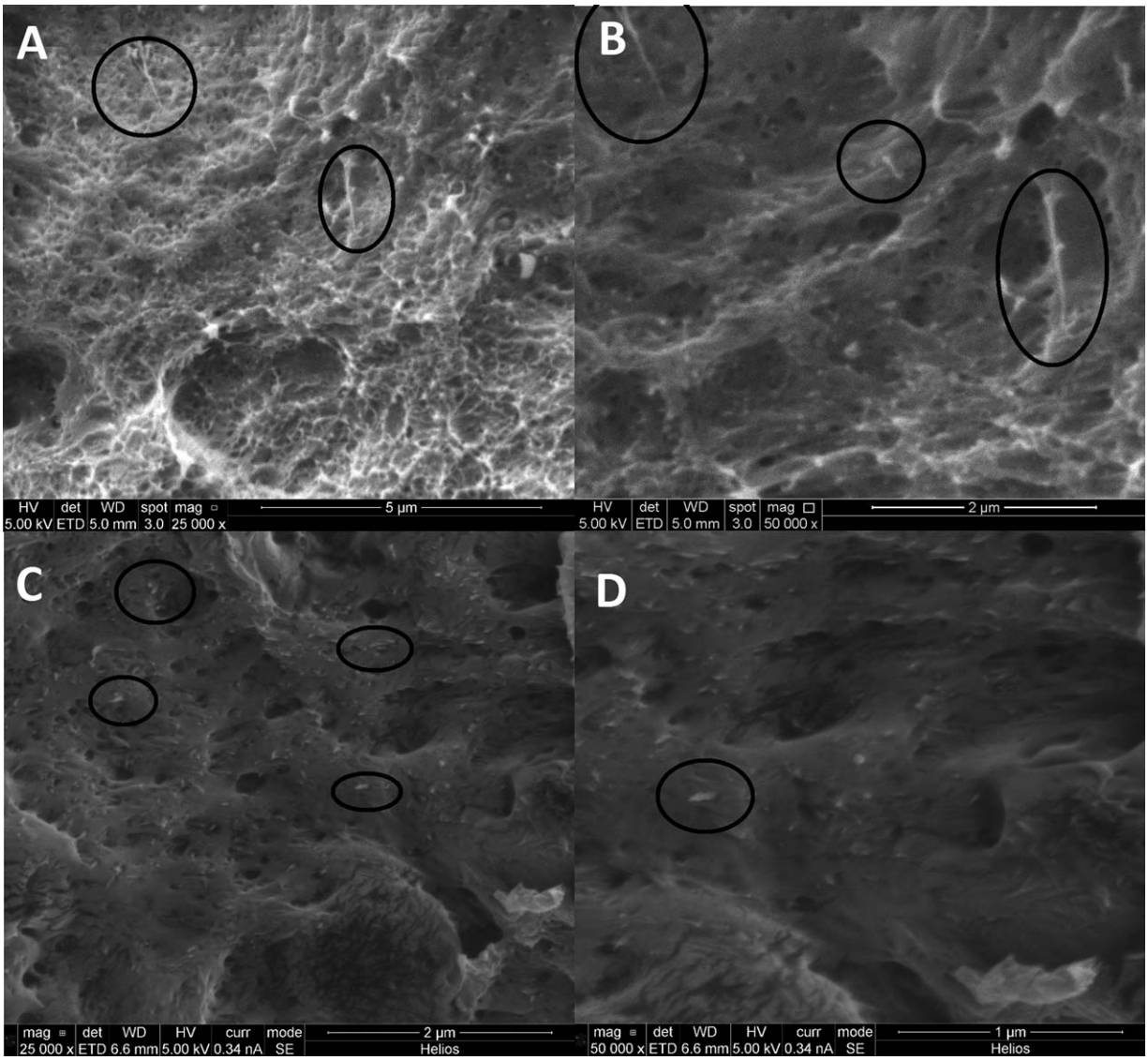

Figure 3. Cross section of PLA/CNF nanocomposites (up) and PLA/CNC nanocomposites (down).

is already a strong treatment that it has already degraded the amorphous domains of the cellulose. Actually, due to those aggressive treatments, it was decided to perform the acid hydrolysis of the CNC at milder conditions to avoid a too high degradation of the cellulose.

Nanocomposite Preparation

For the film making process a critical point was the choice of solvents. The C30B-based nanocomposites were made using DCM as solvent; the reason is that C30B is a hydrophobic clay so it has more affinity with hydrophobic solvents, and there are many reports on using DCM to disperse the C30B in the literature.

For nanocellulose-based nanocomposites it was found that it was not possible to achieve a good dispersion of CNF using DCM, so another solvent was required in order to make a fair comparison between clay and nanocellulose (good dispersion vs. good dispersion). After comparing different solvents (DCM, acetone/DCM, THF, DMF, DMAc, and NMP) it was found that the DMF (dimethylformamide) was the most suitable solvent although the DMAc was showing well dispersed composites too.

Nanocomposite Dispersion Study

In Figure 3 the SEM images of PLA/CNF and PLA/CNC nanocomposites are shown, where no large aggregates within the matrix can be observed for any of the nanocellulose entities. Furthermore, in Figure 3, some individualized CNF and CNC can be observed, proving that we have successfully dispersed the CNF within the matrix. In general, not very clear differences could be observed between CNF and CNC although the CNF is partially acetylated. The authors attribute this effect to the fact that the DMF is a very good solvent for the nanocellulose, (both nanofillers showed a stable dispersion at 1% on DMF), so, the compatibilizing effect of the acetate groups is negligible in this case.

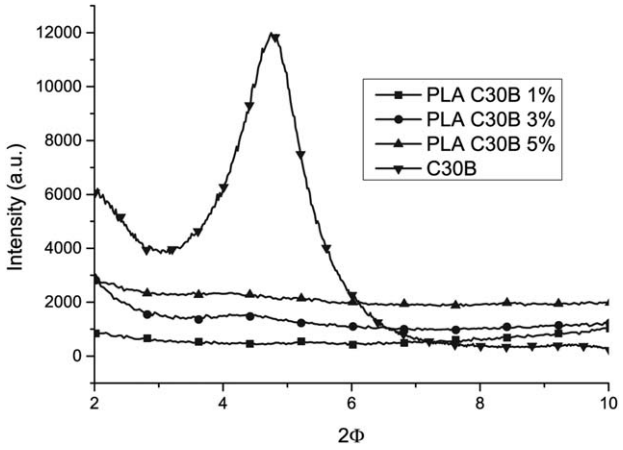

Figure 4. XRD pattern of PLA C30B based nanocomposites.

From the XRD pattern (Figure 4) it can be observed that the peak of neat C30B at ($2\phi = 4.8$), which correspond to the *d*-spacing of the clay, almost disappears in the nanocomposites, especially at 1% load. The absence of a peak means that there is not a constant distance between clay platelets, suggesting that there aren't large aggregates of clay, hence suggesting that there is a good dispersion of clay within the matrix. Moreover, from the TEM images (some representative images could be found on Figure 5) it can be seen that the clay is well dispersed with no evidence of large aggregates.

Crystallinity

Polymer crystallinity is reported to play an important role in determining mechanical and barrier properties.[31,32] Thus, describing the degree of crystallinity of the nanocomposites is critical in terms of extracting conclusions about nanocomposite properties.

All of the nanocomposites showed higher degrees of crystallinity than neat PLA and no significant changes were observed in T_g or T_m. None of the films showed crystallization peaks during the cooling and the heating/cooling/heating procedure. In Figure 6, the degree of crystallinity of the composites is shown and as can be seen that all of the nanocomposites—except

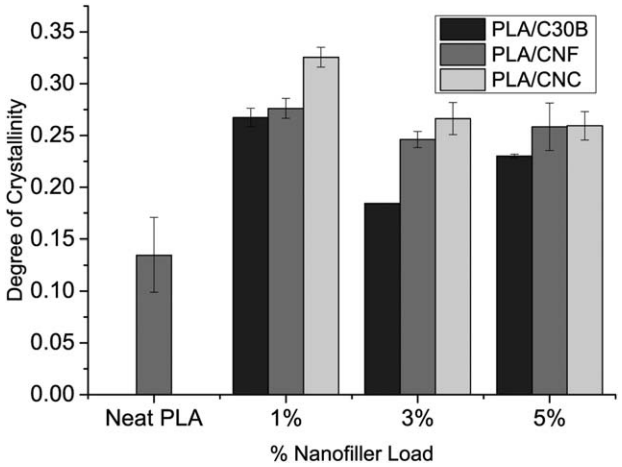

Figure 6. Degree of crystallinity of the nanocomposites (from the 1st heating cycle).

PLA/C30B 3%—have a similar degree of crystallinity, making the nanocomposites at those loads very suitable for comparison.

As previously explained, the slow crystallization time of PLA is a drawback for the industrial application of this polymer, so the addition of fillers that could enhance the crystallization rate would be an important improvement. The nanoclay, the cellulose nanofibers, and nanocrystals[18,33] have been reported to be nucleating agents for PLA thus influencing the crystallization kinetics. To compare the nucleating agent behaviour, the isothermal crystallization process of PLA and the nanocomposites at 1% load at 120°C was studied. The nanocomposites at 1% load were chosen since they had the best dispersion and therefore should be less influenced by the presence of aggregates.

As can be seen in Figure 7, all of the nanocomposites show an endothermic peak shifted to shorter crystallization time. In the case of CNF and CNC, it seems that they show similar crystallization behavior, and slower crystallization kinetics than when using the C30B as an additive. Finally, all of the nanocomposites and the neat PLA reached approximately the same degree

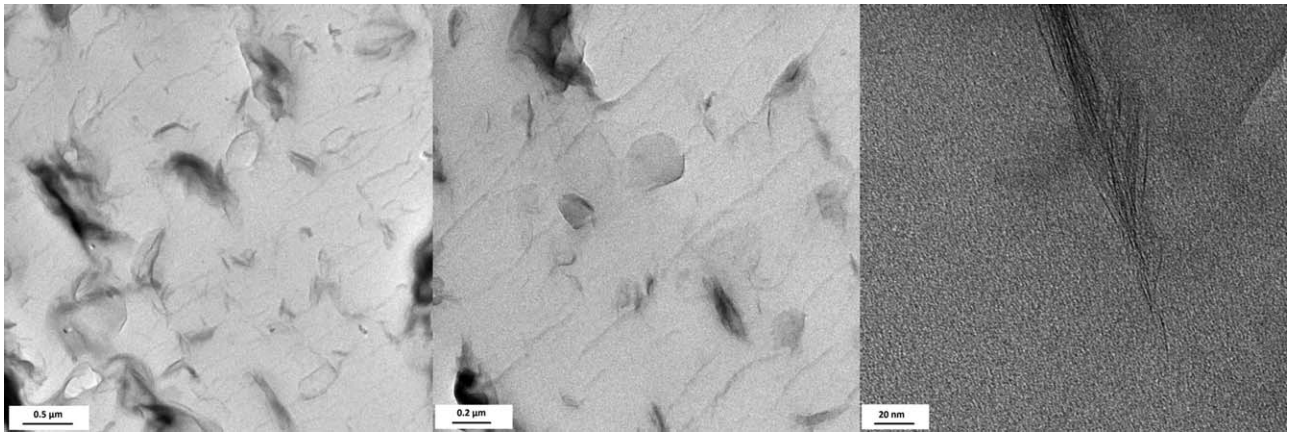

Figure 5. TEM of PLA/C30B 5% Nanocomposite.

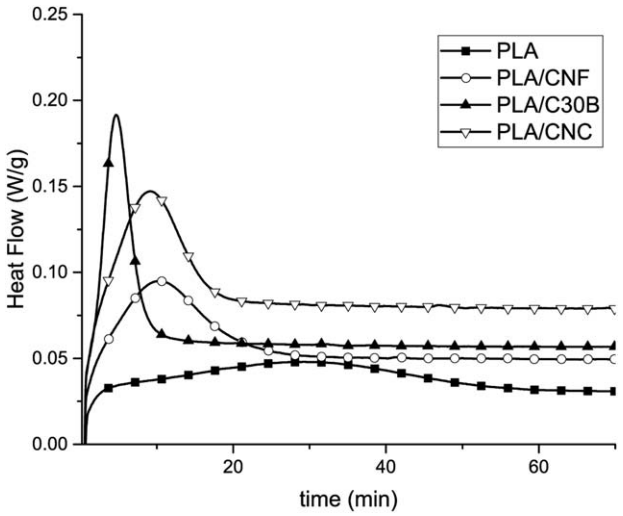

Figure 7. Isothermal crystallization of the nanocomposites at 120°C.

of crystallinity after the isothermal crystallization process (between 35 and 38%).

The results for the clay as nucleating agent is due to the clay platelets—if well dispersed—having much better aspect ratio than nanocellulose-based entities. While the nanocelluose obtained with this method is around 20 nm diameter and 550 nm length, the platelets montmorionite are around 400 nm × 300 nm and few nanometers of thickness if well dispersed, so providing more nucleating sites thus leading to faster crystallization.

The crystallinity is a very complex phenomenon and although it has been classically studied by DSC, this technique does not give all the relevant information. For that reason, polarized optical microscopy (POM) was applied to obtain more information about the spherulite size and distribution.

Briefly, it was found that while PLA and PLA/C30B composites showed a crystalline morphology where was difficult to distinguish the spherulites, the PLA/CNF and PLA/CNC showed a crystalline morphology where the spherulites could be clearly distinguished. Furthermore, the polarized optical micrographs of the samples after isothermal crystallization procedure at 100°C can be found on the Supporting Information. A further study underway to elucidate the influence of the crystalline morphology on the mass transport properties of the film is going to be subject of incoming publications.

Optical Properties

The optical properties of the nanocomposites have not been as widely studied although they are relevant in the case of the food packaging applications. For many applications the industry requires transparent and colorless films. An opaque film will not allow the customer to see the food, making it less likely that the consumer will buy it and a yellow film can give food an artificial color.

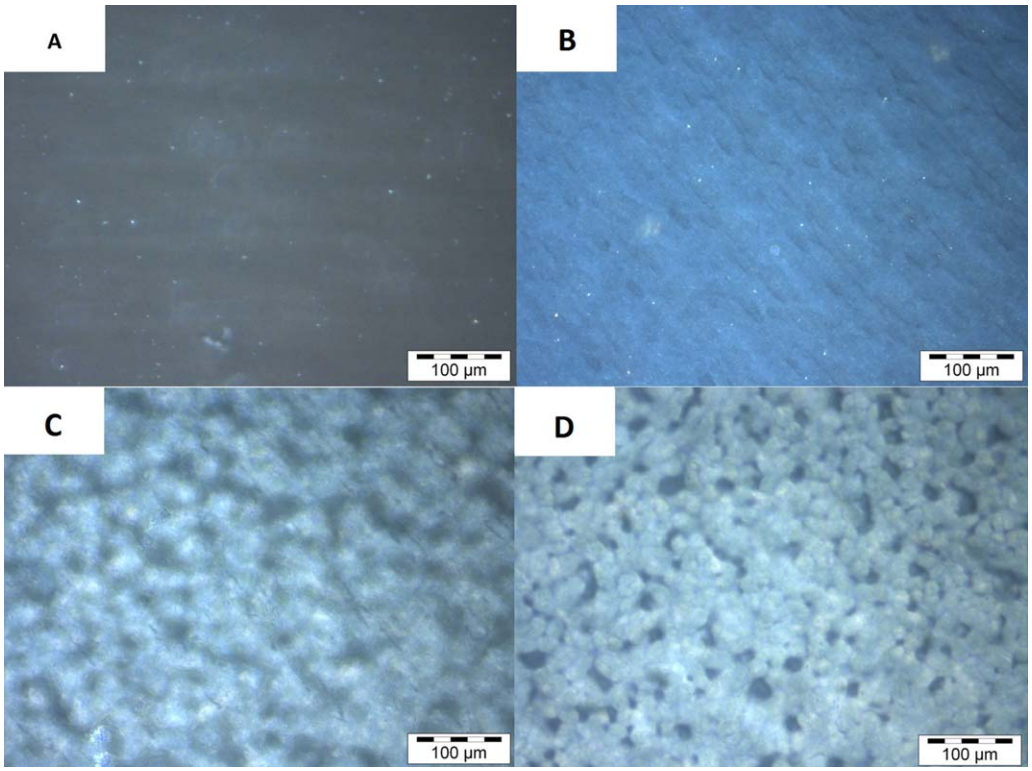

Figure 8. POM of the (A) PLA, (B) PLA/C30B 1%, (C) PLA/CNF 1%, and (D) PLA/CNC 1% films after solvent casting. [Color figure can be viewed in the online issue, which is available at wileyonlinelibrary.com.]

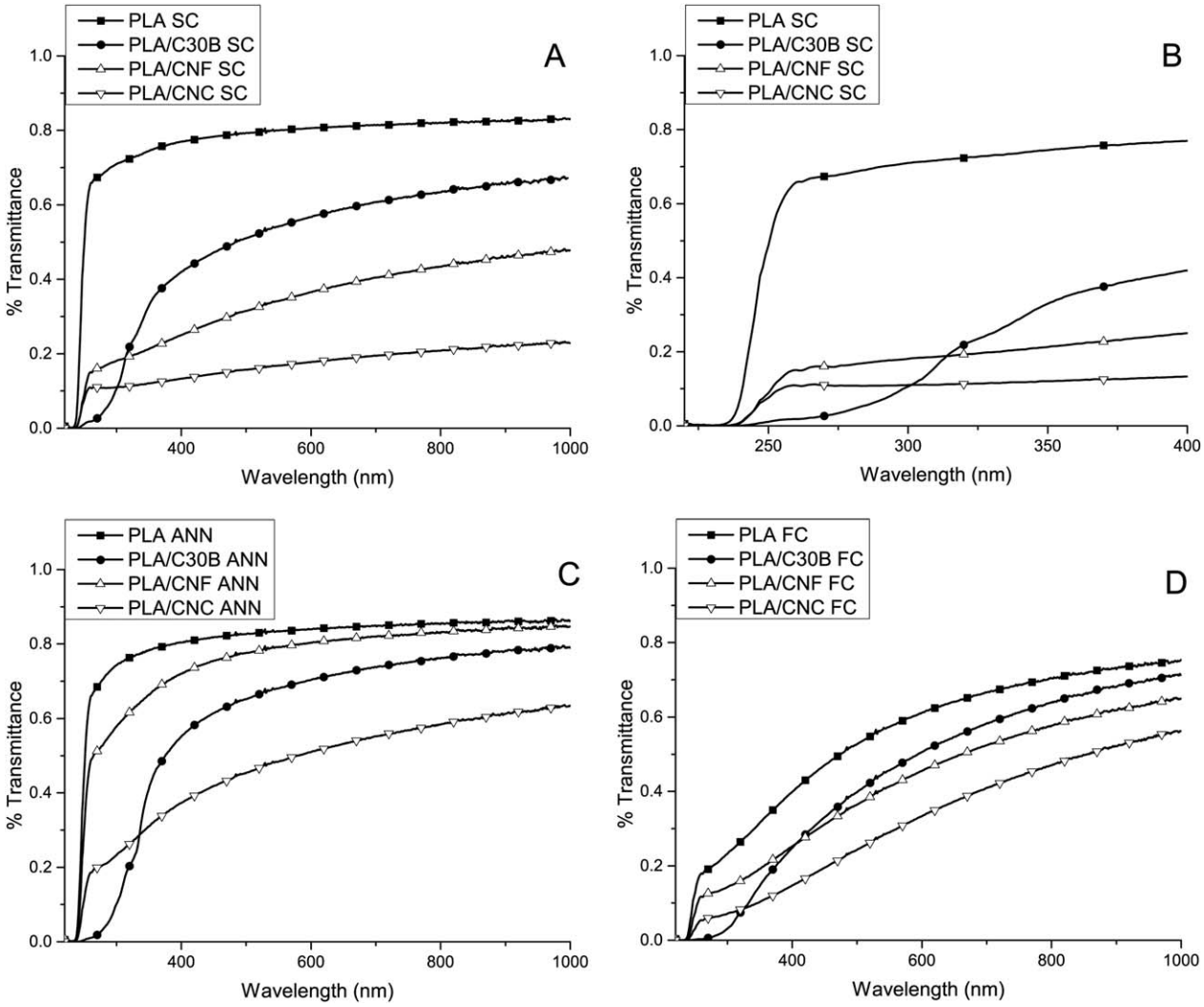

Figure 9. Transmittance of the nanocomposites at 1% filler after solvent casting (A) and (B), after annealing (C) and after isothermal crystallization (D).

As shown in Figure 8 the composites prepared by solvent casting (SC) showed a different crystalline morphology. To eliminate the differences the films prepared by solvent casting were hot pressed for 5 min at 170°C followed by a fast cooling in order to achieve essentially amorphous nanocomposites (AM). After that the annealed nanocomposites were placed into an oven at 120°C for 2 h in order to obtain fully crystallized nanocomposites (FC).

The UV–vis spectroscopy of the samples can be found in Figure 9. All of the samples showed a standard deviation below 10% on absorbance.

From the data it can be seen that the nanocomposites made by solvent casting show reduced transparency compared to the neat PLA film [Figure 9(A,B)]. However, after annealing and isothermal crystallization processes [Figure 9(C,D)] the difference is smaller; probably due to the fact that while after solvent casting procedure (SC) there is a large difference between PLA and nanocomposites in terms of degree of crystallinity (Figure 6); this difference is negligible for annealed (AM) or fully crystallized composites (FC). So, it can be concluded that the addition of small amounts of C30B or CNF doesn't affect significantly the optical properties of the films.

From Figure 9(B) it can be seen how C30B shows a UV blocking capability, which can be desirable in some food packaging applications.[34]

Finally, there is a big difference between annealed [Figure 9(C)] and fully crystallized composites [Figure 9(D)] being the annealed composites more transparent than the fully crystallized ones. This is due to differences in refractive indexes between crystalline and amorphous domains. This difference can be mainly seen on the range of 220–500 nm. The fact that PLA/CNF SC and PLA/CNC SC composites (big spherulite size) show a similar behavior than the fully crystallized composites (big spherulite too), while PLA SC and PLA/C30B SC (small spherulites) show a similar behavior to the quenched composites (no spherulites), suggest that spherulite size has a slight influence on the optical properties of the nanocomposites.

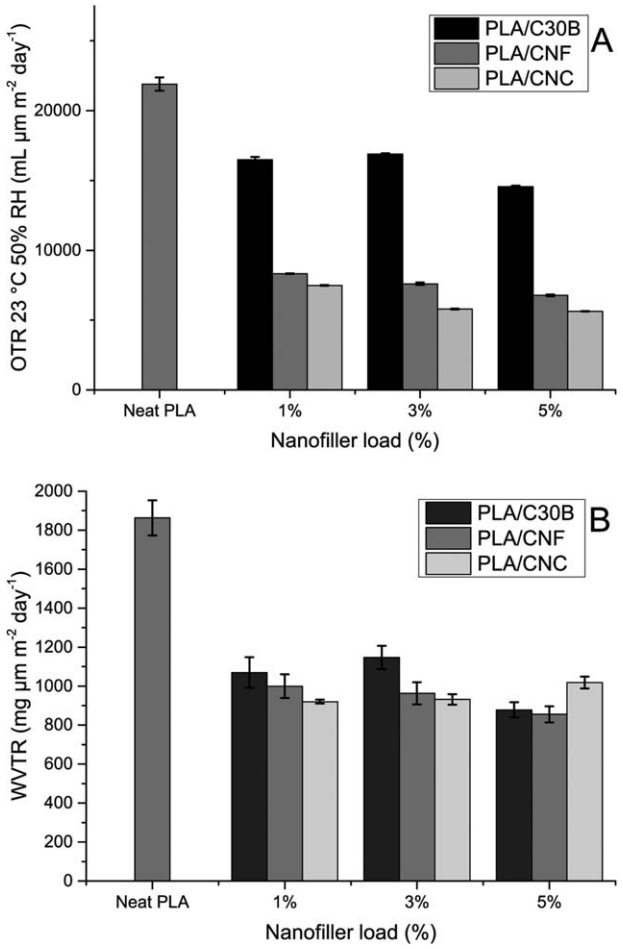

Figure 10. OTR and WVTR of PLA and nanocomposites at 23°C and 50% or RH.

Barrier Properties

Generally the permeability results for PLA and PLA/C30B-based nanocomposites were comparable to those found in the literature either for WVTR[35] or for OTR.[30,34] For PLA/CNF-based nanocomposites there are, to the knowledge of the authors, no other publication using those particular partially acetylated CNF describing barrier properties, but, in the case of CNC, as explained in the introduction, various values for oxygen and water barrier properties can be found in the literature.

In Figure 10, the OTR and WVTR of the neat PLA and its nanocomposites at 23°C and 50% RH can be seen. The results of the OTR at 23 and 0% RH can be found in the Supporting Information.

As can be clearly observed in Figure 10(A) all of the nanocomposites showed better barrier properties than the neat PLA, which could be attributed partially to the fact that the composites showed higher degree of crystallinity than the neat PLA. Surprisingly, nanocellulose-based composites showed lower oxygen transmission rate than nanoclay-based composites. Figure 10(B) also show a great reduction in the WVTR of composites, but, in this case it can be seen that all three nanofillers showed similar behavior, meaning that nanoclay has better performance reducing the WVTR than OTR while CNF has better performance reducing the OTR rather than WVTR. This is probably due to the fact that the clay is likely more hydrophobic than nanocellulose. Finally, In general it can be seen that the addition of nanofillers to PLA matrix is a very promising way to enhance the barrier properties.

The reason of the improvement on the barrier properties could be partially due to the increased crystallinity of the nanocomposites due to the nucleating agent behavior, while the difference between CNF and C30B could be partially due to the different crystalline morphology. A further study underway to elucidate the influence of the nanofillers and crystalline morphology on the mass transport properties of the composites is going to be subject of incoming publications.

Mechanical Properties

The mechanical properties are critical for food packaging applications, since the packaging has to protect the food from damage during the whole supply chain. Although the Young modulus and stress at break of PLA are adequate for food packaging the neat PLA is still too brittle for some food packaging applications, although a range of novel formulations of PLA are now available. Mechanical tests were performed for PLA and its nanocomposites to check the effect of each of the nanofillers on the mechanical properties. The results can be seen in Supporting Information Table I-SI and the values for PLA were in the range of other reports.[15,36] In this work we have found that although the addition of nanofiller did not affect dramatically the mechanical properties of the nanocomposites; PLA/CNF composites showed a slightly better performance than the other nanofillers. The PLA/CNF 1% nanocomposite showed around a 10% of improvement in terms of elongation and stress at break while a 5% loss on Young modulus. Although the mechanical properties, despite the brittleness, of PLA, the low thermomechanical stability keeps the thermoforming of PLA a challenge for the industry. Moreover, there are some food applications that require higher thermal stability of PLA such as disposable glasses for hot drinks. The thermomechanical resistance was investigated by DMA as shown in Figure 11.

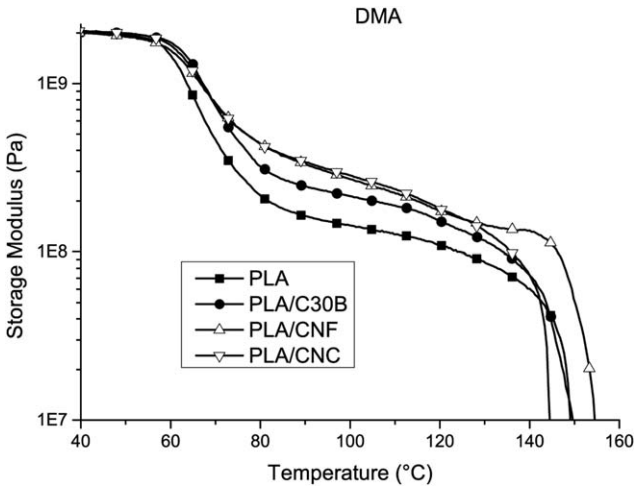

Figure 11. DMA of the nanocomposites.

As can be seen in Figure 11, there is a clear improvement in the thermomechanical properties of PLA and the nanocomposites when surpassing the T_g of PLA. After this point, the mechanical properties of the neat PLA decreases very rapidly whereas the nanocomposites offer greater resistance; this being more pronounced for CNF reinforced composites than for C30B reinforced ones. We ascribed this to the fact that nanocellulose can make stronger percolated networks while the reinforcement of the clay—due to stress transfer mechanism—is not as effective. There is little difference between the effect of CNF and CNC probably due to the fact that CNF is expected to be better dispersed; CNC can form stronger percolated networks due to stronger hydrogen bonding interaction between fillers. Finally, to the understanding of the authors the differences in crystallinity can be neglected in this case since all of the samples were preheated for 20 min at 110°C.

CONCLUSIONS

The performance of a partially acetylated novel CNF as filler for PLA for food packaging applications was compared with the neat PLA and other nanofillers such as clay (C30B) and nanocrystalline cellulose (CNC). It was found that the addition of only a 1% of CNF lead to significant improvements on the performance of PLA for food packaging (a 64% of decrease on oxygen transmission rate, a 46% of decrease on water vapor transmission rate and significant improvement in thermomechanical properties and crystallization kinetic, without a significant influence on the transparency of the films), although part of this improvement could be due to the increased crystallinity present in the nanofillers due to the nucleating agent affect. Comparing CNF with C30B as reinforcing agent, it can be seen how nanocellulose, apart from being biodegradable while clay it is not, has a much better performance than the clay as oxygen barrier, a slightly better performance in thermomechanical and water barrier properties, making this nanofiller a promising candidate for food packaging applications.

ACKNOWLEDGMENTS

The author is thankful to the FP7 - People - 2011, ITN Marie Curie International Training Network (ITN) for the financial support and to COST Action FP1003. The authors wanted to acknowledge Lars Schulte for making the electron microscopies, and Francis Clegg and Christopher Breen for the XRD analysis. This article is on memoriam of Professor Iñaki Mondragon Egaña whose dedication for the science is inspiration for us. LGP2 is part of the LabEx Tec 21 (Investissements d'Avenir - grant agreement n°ANR-11-LABX-0030) and of the Énergies du Futur and PolyNat Carnot Institutes (Investissements d'Avenir - grant agreements n°ANR-11-CARN-007-01 and ANR-11-CARN-030-01).

REFERENCES

1. Available at: http://www.foodproductiondaily.com/Packaging/PLA-bioplastics-production-could-hit-1m-tonnes-by-2020-nova-Institut (Accessed August 2015).
2. Available at: http://www.marketsandmarkets.com/Market-Reports/polylacticacid-387.html (Accessed August 2015).
3. Madhavan Nampoothiri, K.; Nair, N. R.; John, R. P. *Bioresour. Technol.* **2010**, *101*, 8493.
4. Rasal, R. M.; Janorkar, A. V.; Hirt, D. E. *Prog. Polym. Sci.* **2010**, *35*, 338.
5. Bogoeva-Gaceva, G.; Avella, M.; Malinconico, M.; Buzarovska, A.; Grozdanov, A.; Gentile, G.; Errico, M. E. *Polym. Compos.* **2007**, *28*, 98.
6. Najafi, N.; Heuzey, M. C.; Carreau, P. J. *Polym. Eng. Sci.* **2013**, *53*, 1053.
7. Abdul Khalil, H. P. S.; Bhat, A. H.; Ireana Yusra, A. F. *Carbohydr. Polym.* **2012**, *87*, 963.
8. Chinh, N. T.; Trang, N. T. T.; Thanh, D. T. M.; Hang, T. T. X.; Giang, N. V.; Quan, P. M.; Dung, N. T.; Hoang, T. *J. Appl. Polym. Sci.* **2015**, *132*, 41690.
9. Fundador, N. G. V.; Iwata, T. *Polym. Degrad. Stab.* **2013**, *98*, 2482.
10. Kasuga, T.; Maeda, H.; Kato, K.; Nogami, M.; Hata, K.; Ueda, M. *Biomaterials* **2003**, *24*, 3247.
11. Le Bras, D.; Stromme, M.; Mihranyan, A. *J. Phys. Chem. B* **2015**, *119*, 5911.
12. Mihranyan, A.; Edsman, K.; Strømme, M. *Food Hydrocolloids* **2007**, *21*, 267.
13. Eichhorn, S. J.; Dufresne, A.; Aranguren, M.; Marcovich, N. E.; Capadona, J. R.; Rowan, S. J.; Weder, C.; Thielemans, W.; Roman, M.; Renneckar, S.; Gindl, W.; Veigel, S.; Keckes, J.; Yano, H.; Abe, K.; Nogi, M.; Nakagaito, A. N.; Mangalam, A.; Simonsen, J.; Benight, A. S.; Bismarck, A.; Berglund, L. A.; Peijs, T. *J. Mater. Sci.* **2009**, *45*, 1.
14. Siqueira, G.; Bras, J.; Dufresne, A. *Biomacromolecules* **2009**, *10*, 425.
15. Kowalczyk, M.; Piorkowska, E.; Kulpinski, P.; Pracella, M. *Compos. A Appl. Sci. Manufact.* **2011**, *42*, 1509.
16. Fortunati, E.; Peltzer, M.; Armentano, I.; Torre, L.; Jimenez, A.; Kenny, J. M. *Carbohydr. Polym.* **2012**, *90*, 948.
17. Sanchez-Garcia, M. D.; Lagaron, J. M. *Cellulose* **2010**, *17*, 987.
18. Pei, A.; Zhou, Q.; Berglund, L. A. *Compos. Sci. Technol.* **2010**, *70*, 815.
19. Espino-Pérez, E.; Bras, J.; Ducruet, V.; Guinault, A.; Dufresne, A.; Domenek, S. *Eur. Polym. J.* **2013**, *49*, 3144.
20. Kose, R.; Kondo, T. *J. Appl. Polym. Sci.* **2013**, *128*, 1200.
21. Fortunati, E.; Armentano, I.; Zhou, Q.; Iannoni, A.; Saino, E.; Visai, L.; Berglund, L. A.; Kenny, J. M. *Carbohydr. Polym.* **2012**, *87*, 1596.
22. Siqueira, G.; Bras, J.; Dufresne, A. *Langmuir* **2010**, *26*, 402.
23. Trifol, J.; Plackett, D.; Sillard, C.; Bras, J.; Hassager, O.; Daugaard, A.; Szabo, P. TAPPI Nano, Vancouver, **2014**.
24. Leszczyńska, A.; Njuguna, J.; Pielichowski, K.; Banerjee, J. R. *Thermochim. Acta* **2007**, *453*, 75.
25. Zaharia, A.; Sarbu, A.; Radu, A. L.; Jankova, K.; Daugaard, A.; Hvilsted, S.; Perrin, F. X.; Teodorescu, M.;

Munteanu, C.; Fruth-Oprisan, V. *Appl. Clay Sci.* **2015**, *103*, 46.

26. Mohapatra, A. K.; Mohanty, S.; Nayak, S. K. *J. Thermoplast. Compos. Mater.* **2013**, *27*, 699.
27. Zaidi, L.; Bruzaud, S. P.; Bourmaud, A.; Médéric, P.; Kaci, M.; Grohens, Y. *J. Appl. Polym. Sci.* **2009**.
28. Duan, Z.; Thomas, N. L.; Huang, W. *J. Membr. Sci.* **2013**, *445*, 112.
29. Oh, S. B.; Kim, Y. J.; Kim, J. H. *J. Appl. Polym. Sci.* **2006**, *99*, 869.
30. Najafi, N.; Heuzey, M. C.; Carreau, P. J. *Compos. Sci. Technol.* **2012**, *72*, 608.
31. Suryanegara, L.; Nakagaito, A. N.; Yano, H. *Compos. Sci. Technol.* **2009**, *69*, 1187.
32. Picard, E.; Espuche, E.; Fulchiron, R. *Appl. Clay Sci.* **2011**, *53*, 58.
33. Frone, A. N.; Berlioz, S.; Chailan, J. F.; Panaitescu, D. M. *Carbohydr. Polym.* **2013**, *91*, 377.
34. Sanchez-Garcia, M. D.; Lagaron, J. M. *J. Appl. Polym. Sci.* **2010**, *118*, 188.
35. Żenkiewicz, M.; Richert, J. *Polym. Test.* **2008**, *27*, 835.
36. Courgneau, C.; Domenek, S.; Guinault, A.; Avérous, L.; Ducruet, V. *J. Polym. Environ.* **2011**, *19*, 362.